The uplift resistance of shallow embedded anchors

La résistance soulevée des ancres enterrées

P. A. VERMEER, Lecturer, Civil Engineering Department, Delft University of Technology, Netherlands
W. SUTJIADI, Student, Civil Engineering Department, Delft University of Technology, Netherlands

SYNOPSIS Results for the uplift capacity of anchors with depth to breadth ratios of up to eight are presented in this paper. The failure mechanism involves approximately straight rupture lines from the anchor plate to the soil surface. Considering results of finite element computations and scale-model tests, the inclination of a rupture line is found to correspond with the angle of dilatancy. For sand this angle is typically in the range between 0° and 20°, depending on the relative density. A simple formula is derived for the uplift capacity. This formula is shown to give good agreement with empirical data of various researchers.

INTRODUCTION

An embedded anchor consists of a plate which is connected to the anchored structure by means of a cable or tie rod. We consider vertical anchors only, as inclined anchors yield almost the same failure load. The anchors are used for transmission towers, bulkheads and at sea for close station keeping. We will consider a rectangular anchor plate in cohesionless soil, but later the extension to circular plates and cohesive soil is discussed. The classification into shallow and deep anchors is theoretical and relates to the limit load (or failure load). Instead of the depth and the limit load we rather use the embedment ratio and the break-out factor:

embedment ratio = H/B
break-out factor = P/BLHγ

H = depth; B = plate breadth
P = limit load; L = plate length
γ = unit weight of soil

Obviously, the break-out factor increases with embedment ratio and the typical relationship is shown in Fig.1. An anchor in the linear or concave range is considered shallow; otherwise the anchor is deep.

At Delft University the deep anchors are studied experimentally, but the shallow anchors are studied theoretically as plenty of experiments have been reported in the literature. The typical feature of shallow anchors is the formation of approximately straight shear bands from the edges of the anchor plate to the soil surface. However, the literature is not fully unanimous on the straightness of the shear bands and some researchers assume trumpetshaped lines. In the following we will only refer to some recent publications; a complete review of previous work is impossible because of the restricted length of this paper. We will show that the inclination of a shear band coincides to the so-called angle of dilatancy. This soil parameter can either be measured in triaxial testing, or calculated from the friction angle at critical density, ϕ_{cv}.

THE ANGLE OF DILATANCY

Shear dilatancy or shortly dilatancy may be described as the change in volume that is associated with the shear distortion of an element of granular material. Here, an element is assumed to be large enough to contain many particles as micro-elements. Consider for instance a pack of spheres arranged in a state of packing as dense as possible. If any shear distortion is applied, the relative positions of the spheres must change, and the total volume of the pack must increase. This volume change is named dilatancy.

A suitable parameter for characterizing a dilatant material is the dilatancy angle ψ. Originally, this parameter was only used for plane deformation. For such situations with $\varepsilon_2 = 0$ it is defined by the equation (Hansen, 1958).

$$\sin\psi = -\frac{d\varepsilon_1 + d\varepsilon_3}{d\varepsilon_1 - d\varepsilon_3} = \frac{d\varepsilon_v}{-2d\varepsilon_1 + d\varepsilon_v} \qquad (1)$$

where the symbol d is used to denote small increments; $d\varepsilon_v$ is the volumetric strain increment which is considered positive for volume increase. We prefer the definition with the volumetric strain as it also holds for triaxial compression tests with $\varepsilon_2 = \varepsilon_3$ (Vermeer and de Borst, 1984). Typical data for sand is shown in Fig.2. Near and beyond peak strength the dilation rate $d\varepsilon_v/d\varepsilon_1$ attains a constant values, which can be used in eq.(1) to calculate the dilatancy angle. For loose sands this angle tends to zero, but values beyond 15° may be found for dense sands.

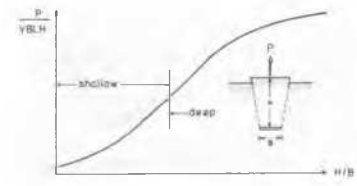

Fig.1

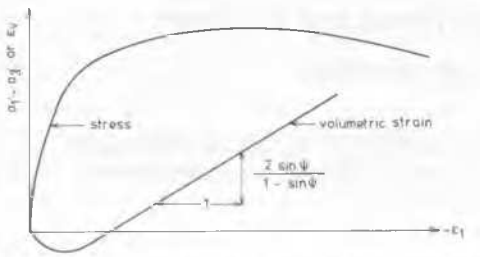

Fig.2 Typical triaxial test data for sand

The meaning of the dilatancy angle is best understood by considering a simple-shear test. Assuming a test with uniform deformation, we have

$$\tan\psi = d\varepsilon_{yy}/d\gamma_{xy} \qquad (2)$$

as illustrated in Fig.3. Hence, ψ is the uplift angle in a simple-shear test or rather in a shear band of arbitrary length.

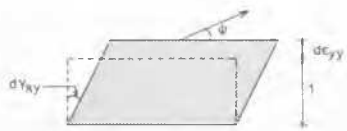

Fig.3

For measuring the dilatancy angle, we recommend a triaxial test rather than a simple-shear test as the latter tends to impose non-uniform stresses in the sample. Instead of a straightforward evaluation from test results, the dilatancy angle may also be calculated from the friction angle by using one of the following equations:

$$\sin\psi = \frac{\sin\phi' - \sin\phi_{cv}}{1 - \sin\phi'\sin\phi_{cv}} \qquad (3a)$$

$$\cos\psi = \frac{\cos\phi'\ \cos\phi_{cv}}{1 - \sin\phi'\sin\phi_{cv}} \qquad (3b)$$

where ϕ_{cv} is the friction angle at the critical state (at the critical density). These equations follow from the stress-dilatancy theory by Rowe (1971). The latter gave both theoretical and empirical evidence for the relationship.

$$\frac{d\varepsilon_v}{d\varepsilon_1} = 1 - \frac{R}{K}, \quad R = \frac{1+\sin\phi'}{1-\sin\phi'}, \quad K = \frac{1+\sin\phi_{cv}}{1-\sin\phi_{cv}}$$

We find the equations (3) by substituting Rowe's relationship in eq.(1).

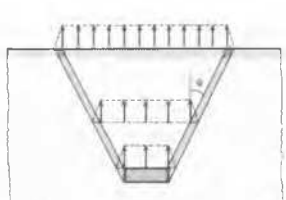

Fig.4 Kinematically admissible failure mechanism

KINEMATICAL SOLUTION FOR PLANE STRAIN

A kinematically admissible failure mechanism for the anchor is shown in Fig.4. A truncated wedge with an apex angle of 2ψ is pulled out together with the anchor plate, which breaks away from the sub soil. Dilating shear bands seperate the truncated wedge from the adjacent soil. Vardoulakis et al.(1981) report a thickness of about 20 times the mean grain diameter. These authors also presented data on the inclination of the shear bands. For a very dense sand with $\phi' = 47^0$ and $\phi_{cv} = 34^0$, the angle with the vertical was measured to be 18^0. This measurement corresponds remarkably well to the dilatancy angle. When using eq.(3a) we obtain $\psi = 17^0$. For a very loose sand the shear bands were found to be vertical. An extremely loose sand is in the so-called critical state with $\phi' = \phi_{cv}$, so that eq.(3a) gives $\psi = 0$. Again this prediction coincides with the observation by Vardoulakis et al.

For $\psi > 0$, the thickness of the shear band increases because of the dilation. However, no material dilates infinitely and the use of a constant dilatancy angle is only a first approximation. In reality the material becomes looser and after intense shearing the critical state with $\phi' = \phi_{cv}'$ is reached. Consider for instance an initially dense sand with a porosity of 36 per cent and $\psi = 17^0$, that dilates to reach the critical state with a porosity of 43 per cent. Then, the shear band thickness increases with 12 per cent. The shear strain that is needed to reach this state is at least 0.4, as can be computed from eq.(2). The value of 0.4 is a lower bound as it is based on the approximation of a constant dilatancy angle, whereas this angle decreases in reality with increase of the porosity. The above exercise leads to the conclusion that the material inside a shear band reaches the critical state when the relative displacement of the shear band boundary is well beyond half the shear band thickness. In other words we need more than 2 mm displacement of the anchor as the thickness of a shear band is about 4 mm. In small-scale model test on rectangular plates we measured less displacement at the limit load, so that the concept of a constant angle of dilatancy is realistic up to and at peak.

For large-scale tests, the concept might be questioned. Near the anchor the displacements may become large, as the truncated wedge does not behave as a rigid block throughout the test. This is best seen from Fig.8 which shows results of finite element computations. Clearly, the shear bands start to develop near the plate and grow up to the surface. In fact, the zone near the plate is sheared very intensively and the dilatancy angle tends to decrease in this region. It would thus seem that the concept of a constant dilatancy angle fails. However, it should be realized that the shear band may displace to "fresh" material. The simplest mechanism would be a shift of the entire shear band into the truncated wedge above the anchor plate. Another mechanism is that only parts of the shear band are shifted inwards, which would result in a curvature of the band. This mechanism seems to prevail as we often observe a slightly trumpet-shaped block above the anchor, rather than exactly straight shear bands.

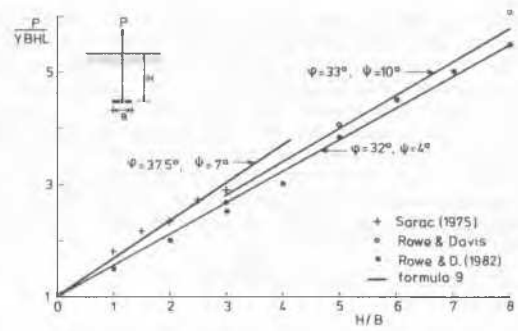

Fig.5 Comparison of experimental and theoretical limit loads. A data point from Rowe represents the average of 5 tests.

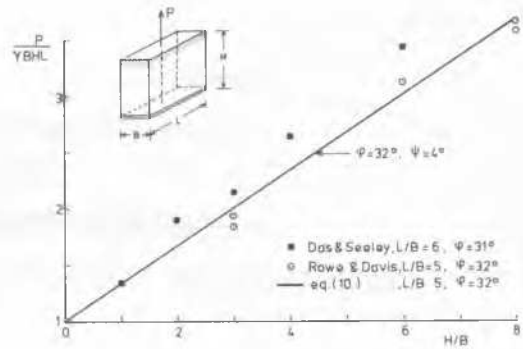

Fig.6 Comparison of experimental and theoretical limit loads.

HAND CALCULATION FOR A LONG STRIP ANCHOR

For estimating the limit load, we need information about the stresses in the soil. In fact, we only need the stresses at the shear bands, say the normal stress σ_n' and the shear stress τ_n. Then, the limit load is calculated from the expressions

$$P = P1+P2+P3, \quad P1 = \gamma BLH, \quad P2 = \gamma LH^2 \tan\psi$$

$$P3 = 2L \int_0^1 (\tau_n \cos\psi - \sigma_n' \sin\psi)\, dl \qquad (4)$$

P1 is the weight of the soil column above the anchor; P2 is the weight of the rest of the truncated wedge; P3 is the shearing resistance and l is the length of a shear band. L/B is assumed to be so large that we can neglect the end effects. Short plates will be consider later (eq.10). From the Mohr-Coulomb criterion we know that $\tau_n < \sigma_n' \tan\phi'$, so that

$$P3 < 2L \int_0^1 \cos\psi(\tan\phi' - \tan\psi')\sigma_n'\, dl$$

Hence, a theoretical upper bound is found by substituting $\psi = \phi'$. Then, P3 vanishes and we obtain

$$P/\gamma BLH < 1 + H/B \tan\phi' \qquad (5)$$

This upper bound is very suitable as a first approximation of the limit load, but we are interested in a better estimate because of the unsafe character of an upper bound.

For deriving an accurate approximation of the limit load we may use (Vermeer and Sutjiadi, 1985)

$$\tau_n = \sigma_n' \tan\alpha \ , \ \sigma_n' = \sigma_v' \qquad (6)$$

where σ_v' is the vertical stress and

$$\tan\alpha = \sin\phi'\cos\psi/(1-\sin\phi'\sin\psi) \qquad (7a)$$

Note that eq.(7a) gives the range $\sin\phi' < \tan\alpha < \tan\phi'$ depending on the dilatancy angle. The lower bound is obtained for a non-dilatant material ($\psi=0$) and the upper bound correspondence to $\psi = \phi'$. The equation for $\tan\alpha$ becomes extremely simple when we eliminate the dilatancy angle from eq.(7a) by using eq.(3), namely

$$\tan\alpha = \tan\phi' \cos\phi_{cv} \qquad (7b)$$

However, for a further evaluation of the limit load it is easier to use eq.(7a). When substituting the eqs (6) and (7a) in eq.(4), we obtain

$$P3 = \frac{\sin\phi' - \sin\psi}{1 - \sin\phi'\sin\psi} L \int_0^1 2\sigma_v'\, dl$$

In order to proceed the evalution, we need an assumption on the magnitude of the vertical force at the shear bands. The simplest assumption is to take the weight P2 of the two triangles above the shear bands. In fact, this assumption is also made in slip-circle analysis for slope stability. It means that we exclude arching by which the centre soil column (P1) may hang on the shear bands. With this assumption the above equation becomes

$$P3 = \frac{\sin\phi' - \sin\psi}{1 - \sin\phi'\sin\psi} \frac{P2}{\sin\psi} \qquad (8)$$

When adding the contributions P1, P2 and P3 the break-out factor is found to be

$$\frac{P}{\gamma BLH} = 1 + \frac{H}{B} \tan\alpha = 1 + \frac{H}{B} \tan\phi' . \cos\phi_{cv} \qquad (9)$$

VALIDATION BY EMPIRICAL DATA

Results of small-scale tests for rectangular anchors are reported by Rowe and Davis (1982.) Their research work is particularly interesting as it includes data on the dilatancy angle, so that we can use eq.(7a). In fact, they published influence charts for use in a hand calculation which include the effect of the dilatancy angle. When comparing the results of the influence-chart-procedure with the formula proposed here, we obtained differences of less than six per cent. For validating our formula, however, we rather consider the results of model tests as shown in Fig.5. We have some doubts about the high dilatancy angle of 10^0, as a sand with $\phi' = 33^0$ tends to be loose and little dilatant. However, the dilatancy angle is only of minor influence as can be seen from the computational results in Fig.5. The dilatancy angle of 7^0 that goes with the data of Sarac (1975) is estimated: it corresponds to $\phi_{cv} = 32^0$.

Fig.6 shows data for shorter anchor plates. The theoretical line comes from the extended formula

$$\frac{P}{\gamma BLH} = 1 + (\frac{H}{B} + \frac{H}{L}) \tan\phi' \cos\phi_{cv} \qquad (10)$$

This formula reduces to eq.(9) when B/L tends to zero, i.e. for an extremely long anchor plate. The theoretical line in Fig.6 is obtained for $\phi' = 32^0$ and $\psi = 4^0$ as given by Rowe and Davis (1982). Das and Seeley (1975) used a sand with a similar friction angle, so that the theoretical line also applies to their data.

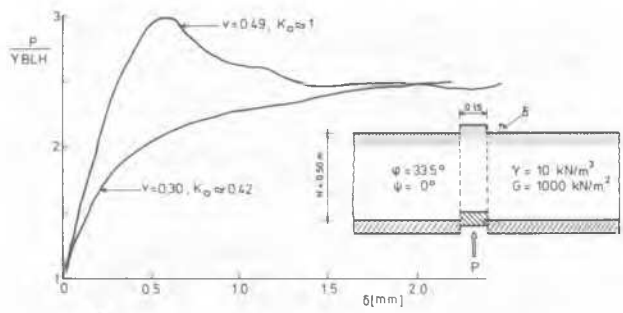

Fig.7 Computed load-uplift curves.

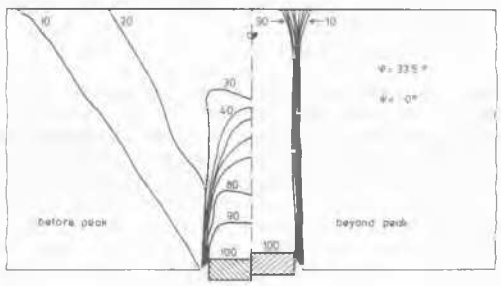

Fig.8 Computed relative velocity contours

VALIDATION BY FINITE ELEMENT COMPUTATIONS

The formules (9) and (10) for the limit load are based on the failure mechanism in Fig.4 and the assumption that the vertical force on the shear band coincides with the soil above. For checking these assumptions, we performed elastoplastic finite element computations. The material model employs an elastic shear modulus and Poisson's ratio and further the constants ϕ',ψ. This so-called perfectly plastic model is among others described in the book by Smith (1982). A special feature of our computer program is the ability to simulate localization of deformation in shear bands (de Borst and Vermeer, 1984).

To facilitate the computations the anchor problem is schematized to a passive trap-door problem. Then the computation proceeds in two stages. First the stresses due to the weight of the soil are computed and subsequently the trap-door is lifted in a number of displacement increments. Fig.7 shows two load-displacement curves for a configuration with H/B = 3.33. With the exception of the Poisson's ratio, all parameters were assigned the same value. For the lower curve we used $\nu = 0.3$ giving a K_o-value of 0.43 at the onset of lifting. In contrast to the lower curve, the upper curve shows a marked peak. This is explained by the use of $\nu = 0.49$ which gives a K_o-value close to unity. The high horizontal stresses cause arching between the shear bands and consequently a high peak load. However, this effect disappears at continued deformation, and a unique residual load is found. Although the K_o-value is found to affect the limit load, K_o is not used in the formulas (9) and (10) as we are interested in the unique residual load rather than an unsafe peak load.

The above computations were performed for a non-dilatant material and we obtained vertical shear bands in both situations (Fig.8). In addition, extremely dilatant material behaviour was considered to observe shear bands at an inclination ψ to the vertical. Obviously, the material model is a rigorous idealisation of real granular material, but it gives an idea of the influence of K_o, the inclination of the shear bands and also on the stresses in the interior of the soil. When summing up the vertical stresses at the shear bands, good agreement was found with the assumption that we made to derive the formulas (9) and (10).

CONCLUDING REMARKS

In the foregoing restriction was made to cohesionless material, but the theory is easily extended to include cohesion. For this purpose, we must use the following relationship between the shear stress and the normal stress at the shear band:

$$\tau_n = (\sigma_n' + c.\ \mathrm{cotan}\phi')\tan\alpha$$

where c is the cohesion and α is defined by eq.(7). Then, it can be derived that

$$\frac{P}{\gamma BLH} = 1 + [(\frac{H}{B} + \frac{H}{L})\tan\phi' + \frac{2c'}{\gamma B} + \frac{2c'}{\gamma L}]\cos\phi_{cv}$$

The dilatancy angle comes in when we use eq.(3b) for ϕ_{cv}. We have shown that the formula is accurate for relatively long plates, say L>3B. For shorter anchor plates and also circular plates, the formula is conservative in the sense that the limit load is underestimated. In the special case of a square anchor with L=B we would have a very simple formula which is also useful for circular anchors as we may use an equivalent breadth. However in such cases the limit load is underestimated due to the neglect of higher order terms in H/B. The extension to include circular anchors is given in another paper by the writers (1985). Finally, it is recalled that the formulas are essentially restricted to shallow anchors. They have been validated for depth to breadth ratios of up to eight.

REFERENCES

de Borst, R. and Vermeer, P.A. (1984). Possibilities and limitations of finite elements for limit analysis. Geotechnique 34, No.2, 199-210.

Das, B.M. and Seeley, G.R. (1977). Uplift capacity of shallow inclined anchors. Proc.9th Int.Conf. Soil Mech.Found.Engg.(1). 463-466, Tokyo.

Hansen, Bent (1958). Line ruptures regarded as narrow rupture zones. Proc.Conf. Earth Pressure Probl.(1), 39-48, Brussels.

Rowe, P.W. (1971). Theoretical meaning and observed deformation parameters for soil. Proc. Roscoe Mem.Symp., 143-194. Cambridge.

Rowe, R.K. and Davis, E.H. (1982). The behaviour of anchor plates, Geotechnique 32, No.1, 25-41.

Sarač, DŽ.(1975). Bearing capacity of anchors. Report 5, Institute of Geotechnics, Sarajewo.

Smith, I.M. (1982). Programming the finite element Method. Chichester, John Wiley & Sons.

Vardoulakis, I., B. Graf and G. Gudehus (1981). Trap door problem with dry sand. Int. J. Numer. Anal. Methods Geomech., 5, 57-78.

Vermeer, P.A. and R. de Borst (1984). Non-associated plasticity for soils, rock and concrete, Heron 29, No.2.

Vermeer, P.A. and Sutjiadi, W. (1985). The behaviour of vertical anchors in soil. To be presented at 4th Int.Conf. Behaviour Offshore Structures, Delft.